IET Circuits, Devices & Systems

Research Article

IET Journals
The Institution of Engineering and Technology

Systematic design approach for a gain boosted telescopic OTA with cross-coupled capacitor

ISSN 1751-858X
Received on 14th November 2016
Revised 25th January 2017
Accepted on 31st January 2017
E-First on 18th April 2017
doi: 10.1049/iet-cds.2016.0448
www.ietdl.org

Ashish Joshi[1], Hitesh Shrimali[1] ✉, Satinder K. Sharma[1]

[1]*School of Computing and Electrical Engineering, Indian Institute of Technology Mandi, Mandi 175005, Himachal Pradesh, India*

✉ *E-mail: hitesh@iitmandi.ac.in*

Abstract: A symbolic analysis is presented to study a gain-boosted telescopic operational transconductance amplifier (OTA) with cross-coupled capacitor (positive feedback) across an auxiliary op-amp. The effects of positive feedback capacitor (PFC) on the pole–zero doublet introduced by the auxiliary op-amp are explored using analytical techniques and simulations. A complete transfer function of the OTA with PFC across the auxiliary op-amp is derived and verified through circuit simulations. The results obtained from circuit simulation and modelled transfer function show good agreement with each other. Furthermore, the analytical expressions for the feedback capacitor in terms of pole–zero locations, unity gain bandwidth (UGBW) and phase margin (PM) are presented. It is shown that UGBW, PM and settling behaviour of the OTA can be tuned by the PFC. A systematic design approach to improve the PM and settling behaviour is discussed. On the basis of the theory presented, 17% improvement in 0.01% settling time is demonstrated.

1 Introduction

The complementary metal–oxide–semiconductor (CMOS) analogue Integrated circuit (IC) design revolves around the fundamental block called operational amplifier (op-amp). Radio subsystems of cell phone, wireless transceivers and data converters are some of the applications where high-speed high-gain op-amps are used [1–4]. The trade-off between power dissipation, number of stages and speed of the operation has motivated a research on single-stage gain-boosted op-amps [5].

Although a typical gain-boosted op-amp has a single-stage architecture, the booster amplifier introduces its own poles and zeros to the overall frequency response. A high-peak occurs in transient analysis resulting in torpid time response because of the pole–zero doublet introduced by the booster amplifier [6–8]. The location of doublet with respect to the unity gain bandwidth (UGBW) decides the settling behaviour [7]. Therefore, the design of booster amplifier turns critical for high-frequency operation. Since it is difficult to isolate the effect of various parameters in circuit, the behaviour and performance of such a complex op-amp is difficult to evaluate in practise directly. Modelling of the amplifier is necessary to understand its small signal behaviour and derive a systematic approach to design a high-performance amplifier [9, 10]. Flandre *et al.* [11] have presented a symbolic analysis of basic gain-boosted operational transconductance amplifier (OTA) to describe the pole–zero doublet behaviour and derive a criteria for optimal settling time. In addition to this, a design criterion to reduce the effect of doublet on settling behaviour of cascode amplifier is reported in [8, 12–15].

Singh *et al.* [16–18] have presented a technique of connecting cross-coupled capacitors across the auxiliary amplifier to obtain better settling behaviour of high-gain, high-speed gain-boosted OTAs. They have demonstrated an application of this technique in 10 bit pipeline and time interleaved successive approximation register (SAR) analogue-to-digital converters in 65 nm technology node [17, 18]. However, the theory and mathematics behind the successful operation of this technique have not been reported. In this paper, the effect of cross-coupled capacitor on booster as well as on the main amplifier is investigated rigorously using analytical techniques and validated through computer simulations. A criterion to choose the value of cross-coupled capacitor C_U is studied and a systematic design approach to design gain-boosted OTA is discussed.

This paper organisation is as follows. A generic model for the gain-boosted op-amp as shown in Fig. 1*a* is developed in Section 2. Section 3 presents the analysis of pole–zero doublet derived in Section 2. Section 4 describes the formulation for systematic design of gain-boosted op-amp depicted in Fig. 1*a*. The simulation results are given in Section 5, followed by conclusion in Section 6.

2 Gain-boosted telescopic op-amp model

In a gain-boosted amplifier, the booster amplifiers employed are generally designed to be of cascode topology to achieve maximum gain at relatively high frequency. A telescopic op-amp with cross-coupled capacitor is considered as an auxiliary amplifier in this paper. The equivalent half circuit used to derive the open-loop transfer function of the gain-boosted op-amp in Fig. 1*a* is shown in Fig. 1*b*. The right-half plane (RHP) zero due to parasitic gate–drain capacitance of the input transistor, M_1, is not considered since its effect is trivial at the moment. The open-loop transfer function, $G(s)$, is obtained as

$$G(s) = \frac{g_{m1} r_{o1} R_D (A_{aux}(s) \cdot g_{m3} r_{o3} - g_{m3} r_{o3} - 1)}{a \cdot s^2 - b \cdot s + c}, \tag{1}$$

$$\begin{aligned} a &= r_{o3} r_{o1} R_D \cdot C_C C_X, \\ b &= R_{CAS} R_D (A_{aux}(s) - 1) \cdot C_X \\ &\quad - r_{o1}(r_{o3} + R_D) \cdot C_C - R_D (r_{o1} + r_{o3}) \cdot C_X, \\ c &= -R_{CAS}(A_{aux}(s) - 1) + r_{o1} + r_{o3} + R_D, \\ R_{CAS} &= g_{m3} r_{o3} r_{o1} \end{aligned}$$

$g_{m1,3}$ and $r_{o1,3}$ are the transconductance and small signal output resistance of the transistors M_1 and M_3, respectively [For an accurate annex, the back-gate effect of transistor where bulk and source are not tied together can be included in the equations by replacing g_m with $(g_m + g_{mb})$, where g_{mb} is the back-gate transconductance of the transistor.], R_D denotes the impedance of the current source I_{REF} which acts as a load for the amplifier. The parasitic capacitance associated with the node C is determined as $C_C = C_{SB3} + C_{DB1} + C_{Aux}$, where C_{Aux} is the capacitance at the input of the auxiliary amplifier. C_X represents the load capacitance

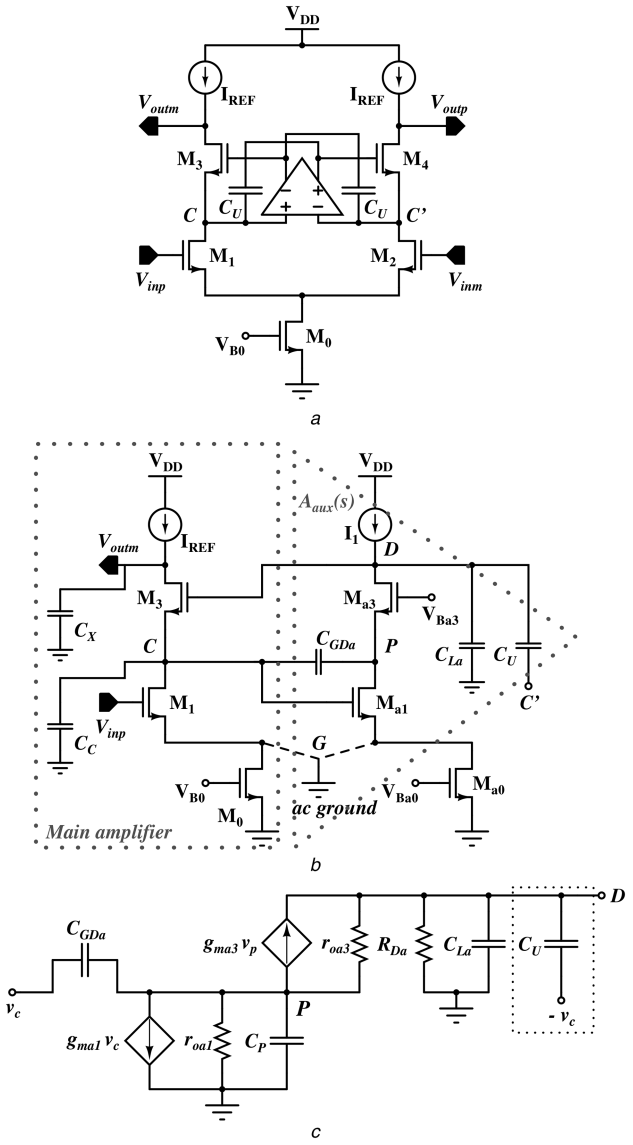

Fig. 1 *Generic model for the gain-boosted op-amp*
(a) Compensation scheme for high-speed, high resolution gain-boosted op-amp, ***(b)*** Half-circuit equivalent of the gain-boosted op-amp as shown in Fig. 1*a*, ***(c)*** Small signal model of the auxiliary op-amp with cross-coupled capacitor C_U [19]

of the amplifier and $A_{\text{aux}}(s)$ is the transfer function of the auxiliary amplifier.

2.1 Auxiliary op-amp with cross-coupled capacitor

The cascode auxiliary amplifier is considered to have a second-order transfer function. To understand the effect of cross-coupled capacitor on the node P, the study of the cascode amplifier considering it as a two pole system becomes necessary from the design prospective. The half circuit of auxiliary op-amp is shown in Fig. 1*b*. The ac small signal model used to analyse the positively closed-loop auxiliary op-amp is shown in Fig. 1*c*. For a differential circuit operation, the ac small signals at the input of auxiliary amplifier are 180° phase shifted with respect to each other, and hence the capacitor C_U is synthesised by connecting it between nodes D and $-v_c$ [19].

The transfer function of the auxiliary op-amp with cross-coupled capacitor is therefore incurred by solving nodal equations for Fig. 1*c*. The simplified transfer function is given by (2)

$$A_{\text{aux}}(s) = \frac{j \cdot s^2 + k \cdot s + l}{x \cdot s^2 + y \cdot s + z} \tag{2}$$

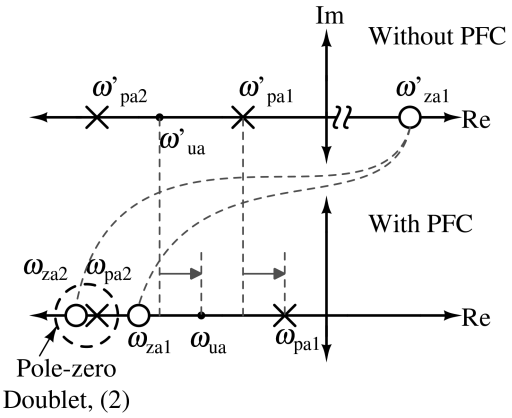

Fig. 2 *Location of poles and zeros, without and with the PFC across the auxiliary op-amp*

$$j = -R_{\text{Da}} r_{\text{oa3}} r_{\text{oa1}} C_U (C_P + C_{\text{GDa}}),$$
$$k = -[R_{\text{Da}} R_{\text{CASa}} (C_U - C_{\text{GDa}}) + R_{\text{Da}} (r_{\text{oa3}} + r_{\text{oa1}}) C_U],$$
$$l = -g_{m\text{a1}} R_{\text{Da}} R_{\text{CASa}},$$
$$x = R_{\text{Da}} r_{\text{oa3}} r_{\text{oa1}} (C_U + C_{\text{La}})(C_P + C_{\text{GDa}}),$$
$$y = [R_{\text{Da}} R_{\text{CASa}} (C_U + C_{\text{La}}) + R_{\text{Da}} r_{\text{oa1}} (C_P + C_{\text{GDa}})],$$
$$z = R_{\text{CASa}} + R_{\text{Da}}$$

The transconductance and small signal output resistance of transistors M_{a1} and M_{a3} are denoted by $g_{m\text{a1, 3}}$ and $r_{\text{oa1, 3}}$, respectively. C_{GDa} and C_{La} are the gate–drain parasitic capacitance of M_{a1} and the load capacitance seen at the output of auxiliary op-amp, respectively, and R_{Da} represents the impedance of the current source I_1. $R_{\text{CASa}} = g_{m\text{a3}} r_{\text{oa3}} r_{\text{oa1}}$ being the impedance of the cascode stage, while deriving (2) and subsequent poles and zeros it is assumed that $R_{\text{CASa}} \gg r_{\text{oa3}}$, r_{oa1}.

Equation (2) suggests that the three capacitors C_P, C_U and C_{La} form a loop giving a second-order transfer function with two poles, ω_{pa1} and ω_{pa2} at frequencies

$$\omega_{pa1} = \frac{1}{R_{\text{OUTa}}(C_U + C_{\text{La}})} \tag{3}$$

$$\omega_{pa2} = \frac{(g_{m\text{a3}} r_{\text{oa1}} + 1)}{r_{\text{oa1}}(C_P + C_{\text{GDa}})} \simeq \frac{gm_3}{(C_P + C_{\text{GDa}})} \tag{4}$$

where $|\omega_{pa1}| < |\omega_{pa2}|$ and $R_{\text{OUTa}} \simeq R_{\text{Da}} || R_{\text{CASa}}$ is the output resistance of the auxiliary op-amp. Furthermore, it can be observed that addition of C_U in the circuit gives a second-order numerator. If capacitance C_P is relatively small, then two real valued zeros are located at frequencies

$$\omega_{za1} = \frac{g_{m\text{a1}}}{C_U - C_{\text{GDa}}} \tag{5}$$

$$\omega_{za2} = \frac{(g_{m\text{a3}} r_{\text{oa3}} + 1)}{r_{\text{oa3}}(C_P + C_{\text{GDa}})} \simeq \frac{gm_3}{(C_P + C_{\text{GDa}})} \tag{6}$$

where $|\omega_{z1}| < |\omega_{z2}|$. Fig. 2 exemplifies the locations of auxiliary amplifier's poles and zeros, without and with the positive feedback capacitor (PFC). Since the dc gain remains constant and the dominant pole moves inside, the positively closed-loop op-amp has relatively small UGBW compared with its open-loop similitude.

From the analysis presented till now, we conclude that the auxiliary op-amp can be reduced to a first-order transfer function, $A_{\text{aux}}(s)$, even when a second-order amplifier is considered at the first place. This is because the capacitor C_U creates a pole–zero pair given by (4) and (6), cancelling the effect of non-dominant

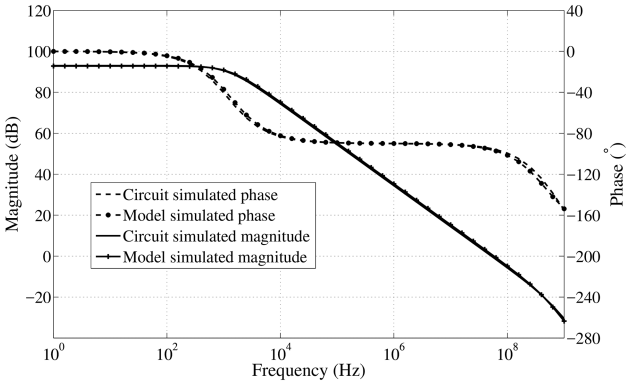

Fig. 3 *Magnitude and phase response of the op-amp when* $g_{m1} = 376\,\mu S$, $g_{m3} = 355\,\mu S$, $r_{o1} = 80\,k\Omega$, $r_{o3} = 21\,k\Omega$, $R_D = 210\,M\Omega$, $A_{dc} = 447$, $\omega_{pa1} = 17.3\,kHz$, $\omega_{za1} = 15.6\,MHz$, $C_C = 3\,fF$, $C_{La} = 48\,fF$, $C_X = 1\,pF$ *and* $C_U = 200\,fF$

pole at the node P on the auxiliary amplifier's frequency response. Therefore, the transfer function of the auxiliary op-amp with the cross-coupled capacitor is written as

$$A_{\text{aux}}(s) = -A_{\text{dc}}\frac{\left[1 + (s/\omega_{za1})\right]}{\left[1 + (s/\omega_{pa1})\right]} \tag{7}$$

where $A_{\text{dc}} = g_{ma1}R_{\text{OUTa}}$ is the dc gain of the auxiliary op-amp.

Substituting (7) into (1) yields a third-order transfer function for the overall gain-boosted amplifier with one left-half plane zero. The transfer function, $G(s)$ is given as (see (8)) From (8), the locations of poles and zeros are incurred to be

$$\omega_{p1} \simeq \frac{1}{R_{\text{OUT}} \cdot C_X} \tag{9}$$

$$\omega_{p\text{d}} \simeq \frac{g_{ma1} \cdot R_{\text{CAS}} \cdot C_X + C_2}{R_{\text{CAS}} \cdot C_X[C_1 + C_2 + ((C_2 \cdot (r_{o1} + r_{o3}))/R_{\text{CAS}})]} \tag{10}$$

$$\omega_{p3} \simeq \frac{g_{m3} \cdot (C_1 + C_2)}{C_C \cdot C_2} + \frac{r_{o1} + r_{o3}}{C_C \cdot r_{o1}r_{o3}} + \frac{1}{r_{o3} \cdot C_X} \tag{11}$$

$$\omega_{z\text{d}} \simeq \frac{g_{ma1}}{C_1 + C_2} \tag{12}$$

$$R_{\text{OUT}} \simeq A_{\text{dc}}R_{\text{CAS}}||R_{\text{D}},\ C_1 = C_U - C_{\text{GDa}},\ C_2 = C_U + C_{\text{La}}$$

where $\omega_{p1} < \omega_{p\text{d}}$, $\omega_{z\text{d}} < \omega_{p3}$. As anticipated, (10) and (12) show the presence of pole–zero doublet in overall amplifier's frequency response.

The pole–zero pair given by (4) and (6) is not considered in the model derivation. Consideration of this pair into the analysis results in an additional high-frequency pole–zero doublet (ω_{dhf}) in the vicinity of ω_{za2}. The location of this doublet is found to be

$$\omega_{\text{dhf}} = \frac{\omega_{\text{ua}}\omega_{pa2}\omega_{za2} + \omega_{pa2}\omega_{za1}\omega_{za2}}{\omega_{\text{ua}}\omega_{pa2} + \omega_{za1}\omega_{za2}} \tag{13}$$

Table 1 Locations of poles and zeros for $C_U = 200\,\text{fF}$

	Circuit simulation, Hz	Model simulation, Hz
ω_{p1}	-1.17×10^3	-1.32×10^3
$\omega_{p\text{d}}$	-4.98×10^6	-5.36×10^6
$\omega_{z\text{d}}$	-4.99×10^6	-5.35×10^6
ω_{p3}	-5.17×10^8	-4.93×10^8

where ω_{ua} is the UGBW of auxiliary op-amp with the cross-coupled capacitor. Generally, ω_{dhf} is located at the frequencies away from the UGBW of the overall amplifier and has a negligible effect on the amplifier's behaviour. Moreover, the theory of substituting (7) as $A_{\text{aux}}(s)$ simplifies the analysis and derivation of the model equation to a great extent. Therefore, it is judicious to ignore (4) and (6) for a systematic design approach.

To validate the above analysis, the op-amp in Fig. 1*a* is designed in a standard 90 nm technology with the supply voltage of 1.5 V and simulated using electronic design automation (EDA) tools. The model equation given by (8) is implemented in MATLAB [20]. The op-amp has dc gain of 93 dB and UGBW of 53 MHz. Fig. 3 compares the magnitude and phase response obtained from both the simulations. From Fig. 3, it is evident that both the results are in close agreement with each other. As shown in Table 1, the locations of poles and zeros obtained from model are found matched with the pole–zero simulation result from EDA tool.

3 Analysis of the doublet

3.1 Effect of C_U on the transient response

The transient response of second-order system when it is connected in unity gain feedback is studied for various cases of poles and zeros locations. An exponential behaviour is observed in the system's response. The exponential response is due to the dominant pole and the location of non-dominant pole is responsible for settling accuracies in high-speed high-gain applications. Therefore, the non-dominant pole decides the maximum speed of a second-order systems.

In the case of gain-boosted op-amp with a pole–zero doublet, the effect of fractional spacing ($\omega_{z\text{d}}/\omega_{p\text{d}}$) between the doublet and its location on the transient response of overall op-amp is illustrated in Fig. 4. Settling accuracy of 0.01% is considered which corresponds to settling to 0.9999 (12 bits resolution for unit step). The magnitude of slow-settling component corresponds to the fractional spacing ($\omega_{z\text{d}}/\omega_{p\text{d}}$) between the doublet. If the doublet is placed outside the UGBW, ω_{u}, of the overall amplifier, reducing the fractional spacing from 1.1 to 1.06 leads to 12.5% reduction in settling time when compared with the second-order settling. On the other hand, reducing the spacing between low-frequency doublet does not help in terms of settling behaviour because its effect persists for relatively longer period with a reduced magnitude.

To understand the nature of poles and zeros present in the overall amplifier's frequency response, $A_{\text{aux}}(s)$ is modified and rewritten as

$$A_{\text{aux}}(s) = -\frac{\left[1 + (s/\omega_{za1})\right]}{\left[(1/A_{\text{dc}}) + (s/\omega_{\text{ua}})\right]} \tag{14}$$

$$G(s) = \frac{\begin{array}{c}-g_{m1}r_{o1}R_{\text{D}}[(A_{\text{dc}}g_{m3}r_{o3}\omega_{pa1} + g_{m3}r_{o3}\omega_{za1} + \omega_{za1}) \cdot s \\ +(A_{\text{dc}}g_{m3}r_{o3} + g_{m3}r_{o3} + 1)\omega_{pa1}\omega_{za1}]\end{array}}{\begin{array}{c}C_CC_XR_{\text{D}}r_{o3}r_{o1}\omega_{za1} \cdot s^3 + [C_Cr_{o1}\omega_{za1}(R_{\text{D}} + r_{o3}) + C_XR_{\text{D}}\{\omega_{pa1}(C_Cr_{o3}r_{o1}\omega_{za1} \\ +A_{\text{dc}}R_{\text{CAS}}) + \omega_{za1}(R_{\text{CAS}} + r_{o3} + r_{o1})\}] \cdot s^2 + [C_Cr_{o1}\omega_{pa1}\omega_{za1}(R_{\text{D}} + r_{o3}) \\ +\omega_{za1}(R_{\text{D}} + r_{o3} + r_{o1}) + R_{\text{CAS}}(A_{\text{dc}}\omega_{pa1} + \omega_{za1}) + C_XR_{\text{D}}\omega_{pa1}\omega_{za1}\{R_{\text{CAS}}(A_{\text{dc}} + 1) \\ +(r_{o3} + r_{o1})\}] \cdot s + \omega_{pa1}\omega_{za1}[R_{\text{CAS}}(A_{\text{dc}} + 1) + R_{\text{D}} + r_{o3} + r_{o1}]\end{array}} \tag{8}$$

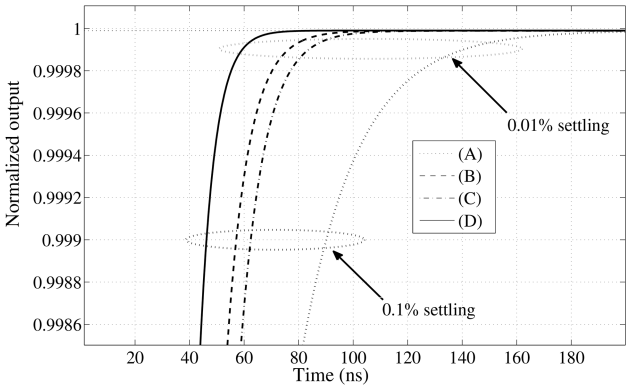

Fig. 4 *Case study: computed unity gain step response for various cases: (A)* $\omega_{zd} = 0.5\omega_u$, $\omega_{zd} = 1.06\omega_{pd}$, *(B)* $\omega_{zd} = 2\omega_u$, $\omega_{zd} = 1.06\omega_{pd}$, *(C)* $\omega_{zd} = 2\omega_u$, $\omega_{zd} = 1.1\omega_{pd}$ *and (D) reference second-order response without pole–zero doublet when location of non-dominant pole* $= 4\omega_u$

substituted in (1) and the result is numerically evaluated considering an example case. The UGBW of auxiliary op-amp ($\omega_{\rm ua}$) is the parameter under consideration. The value of input transconductance of the auxiliary op-amp is approximated as $g_{ma1} \simeq \omega_{\rm ua}(C_U + C_{\rm La})$ to calculate the zero location corresponding to each $\omega_{\rm ua}$. This numerical approach is illustrated in Fig. 5. From this figure, it can be noted that the unity gain frequency of the auxiliary op-amp when $\omega_{p\rm d}$ and ω_{p3} have merged to become complex conjugate poles is less in case (b) where PFC is connected across the auxiliary op-amp. The pole–zero doublet without the PFC [Note that the locations of poles and zeros without the PFC can be obtained by putting $C_U = 0$ in (9)–(12), if a single pole roll off is assumed for the auxiliary op-amp. This also proves the significance of the proposed symbolic analysis.] fall in the locale of the UGBW of auxiliary amplifier; a result in accordance with intuitive analysis presented in [7]. This implies that the quality of transient response in this case depends on the location of UGBW of auxiliary amplifier. However, from (10) and (12), it can be observed that the addition of PFC across the auxiliary amplifier gives a pole–zero doublet which strongly depends on the value of C_U. The effect of C_U on the magnitude of slow-settling component can be understood by calculating the relative error in the pole and zero doublet frequencies. Assuming $g_{ma1}R_{\rm CAS}C_X > C_2$ in (10)

$$\frac{\omega_{z\rm d} - \omega_{p\rm d}}{\omega_{\rm u}} = \frac{g_{ma1} \cdot k_{\rm r}C_2 \cdot C_X}{g_{m1}(C_1 + C_2 + k_{\rm r}C_2)(C_1 + C_2)} \tag{15}$$

where $k_{\rm r} = (r_{\rm o1} + r_{\rm o3})/R_{\rm CAS}$ is a constant. From (10), (12) and (15) it is evident that increasing the value of C_U will push the doublet to a lower frequency and have smaller magnitude of slow-settling component compared with the doublet without C_U. Hence, the settling accuracy can be tuned by the cross-coupled capacitor.

3.2 Phase margin (PM) and the stability

3.2.1 Stability of internal feedback loop: It is necessary to check the internal stability of the gain-boosted op-amp when the PFC is connected across the auxiliary amplifier. The closed-loop transfer function ($A_{\rm CL}$) of the auxiliary op-amp can be written as

$$A_{\rm CL}(s) = -A_{\rm dc} \cdot \frac{\left[1 + (s/\omega_{z\rm a1})\right]\left[1 + (s/\omega_{z\rm a2})\right]}{\left[1 + (s/\omega_{pc\rm a1})\right]\left[1 + (s/\omega_{pc\rm a2})\right]} \tag{16}$$

$$\omega_{pc\rm a1} = \frac{\omega_{pa1}\omega_{z\rm a1}(1 + A_{\rm dc}\beta)}{\omega_{z\rm a1} + A_{\rm dc}\beta\omega_{pa1}}, \quad \omega_{pc\rm a2} \simeq \omega_{pa2}$$

where β is the internal feedback factor, $A_{\rm aux}(s)$ is the transfer function of auxiliary op-amp considering the pole–zero pair given

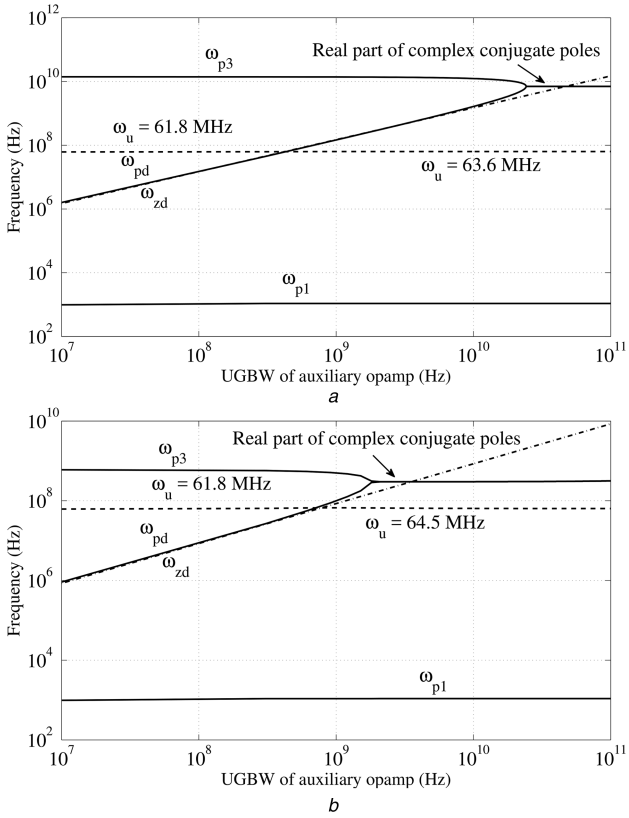

Fig. 5 *Pole-zero frequency locations of the overall amplifier*
(a) Without PFC, ***(b)*** With PFC of 200 fF across the auxiliary op-amp; for $g_{m1} = 400\,\mu$S, $g_{m3} = 400\,\mu$S, $r_{\rm o1} = 80\,$kΩ, $r_{\rm o3} = 30\,$kΩ, $R_{\rm D} = 210\,$MΩ, $A_{\rm dc} = 500$, $C_{\rm La} = 50\,$fF, $C_X = 1\,$pF, $C_{\rm GDa} = 700\,$aF and $C_{\rm C} = 5\,$fF $+ C_U$

by (4) and (6), $\omega_{pc\rm a1}$ and $\omega_{pc\rm a2}$ are the closed-loop poles such that $\omega_{pc\rm a1} < \omega_{pc\rm a2}$. Equation (16) indicates that the internal feedback loop is stable even when the worst-case feedback ($\beta = 1$) is considered. To understand this, recall from (7) that for practical assumption of $C_U > C_{\rm GDa}$, RHP zero because of the parasitic gate–drain capacitance of auxiliary op-amp moves to the left half of complex plane such that $\omega_{z\rm a1} > \omega_{\rm ua}$. Existence of this zero in the transfer function prevents internal feedback loop from instability. The zero starts to provide additional positive phase about a decade before its actual occurrence and improves the PM of the auxiliary op-amp.

3.2.2 Phase margin: The PM of overall amplifier depends on the doublet location and the excess phase, $\Delta\phi$, introduced by the doublet. The excess phase can be related to the fractional spacing between the doublet by the following equation:

$$\Delta\phi = \arctan\left(\frac{\omega_{\rm u}\omega_{p\rm d}(1-\gamma)}{\omega_{\rm u}^2 - \gamma\omega_{p\rm d}^2}\right) \tag{17}$$

where the fractional spacing between the doublet (γ) can be calculated as

$$\gamma = \frac{\omega_{z\rm d}}{\omega_{p\rm d}} = 1 + \frac{C_U + C_{\rm La}}{2C_U + C_{\rm La}} \cdot k_{\rm r} \tag{18}$$

The spacing between the doublet, and therefore the excess phase reduces when PFC is connected across the auxiliary amplifier. Maximum reduction in the spacing is approximately limited to $(50k_{\rm r}/k_{\rm r} + 1)\%$ when compared with the spacing without C_U. As $\Delta\phi$ decreases the PM increases. Conceptually, this can be understood by noting that C_U brings the doublet frequencies closer to each other, thereby minimising the deviation of ac response from ideal two pole system's ac response.

4 Formulation for systematic design approach

Fractional spacing between the doublet decreases with increment in C_U. As a result, magnitude of slow-settling component further reduces; however, the time constant of the slow-settling component increases. Therefore, while selecting C_U, the location of ω_{zd} and PM of the auxiliary amplifier must be considered along with the area constraints. A design approach is presented here by considering C_U as one of the design parameter available for designers. Transient and phase response are discussed separately.

4.1 Transient response

Numerical methodology and computer simulations show that placing the doublet within 1.4–3 times the ω_u for 80–90° PM of the auxiliary op-amp exhibits a good settling behaviour when $\gamma = 1.06$ and settling accuracy of 0.01% are considered. Settling to 0.1% is also studied for the completeness and it is found that $\gamma = 1.06$ results in a peak amplitude which stays in the error band when the doublet is placed within 2–2.5 times the ω_u for more than 85° PM of the auxiliary op-amp. $\gamma = 1.06$ is chosen considering $k_r = 0.1$ and $n = (C_U/C_{La}) = 2$. However, in typical designs k_r ranges from 0.03 to 0.07 and hence placing the doublet within aforesaid range will not degrade the results in practical designs. Reduction in k_r can be achieved by increasing the intrinsic gain ($g_m r_o$) of the cascode transistor M_3. Hence, in the first version of the design, length of M_3 is usually increased to increase the resistance and proportionally wide transistor be designed to improve voltage headroom. The UGBW of auxiliary op-amp required for this placement of the doublet is given as: $\omega_{ua} = (2n+1)\omega_{zd}/(n+1)$. Therefore, the current I_1 for the first version design can be calculated from the transconductance required to place the doublet at particular location. The minimum achievable settling time depends on the given power budget. More the PM of auxiliary op-amp higher will be the power.

4.2 Frequency response

Equation (19) relates the PM of overall amplifier to the poles and zeros locations where $\theta = \omega_{p1}/\omega_u$, $\eta = \omega_{p3}/\omega_u$ and PM is the phase margin of overall amplifier

$$\frac{\theta+\eta}{1-\theta\eta} = \tan(\mathrm{PM} - \Delta\phi) \tag{19}$$

The UGBW of auxiliary op-amp without cross-coupled capacitor is given as $\omega'_{ua} \simeq g_{ma1}/C_{La}$. After connecting the PFC, the doublet with fractional spacing of $1 + k_r(n+1)/(2n+1)$ will fall close to $\omega'_{ua}/(2n+1)$. The input transconductance of auxiliary op-amp, g_{ma1}, is required to be sufficiently high to accommodate the reduction in the UGBW from ω'_{ua} to ω_{ua} ($\omega_{ua} = \omega'_{ua}/(n+1)$).

Considering all these facts, a systematic design approach can be explained as follows:

i. Design a cascode amplifier with desired UGBW and PM higher than 65°. Calculate the value of C_{La}. In amplifiers optimised for high-speed and low-power applications, the load capacitance of auxiliary op-amp ($C_{La} = C_{GS3} + C_{GD3}$) is comparable with the capacitance at node C (see Fig. 1).
ii. Decide the location of the doublet depending on the required settling performance and power budget. At this stage, it is assumed that the PM of auxiliary amplifier (PM_a) is ≥80°.
iii. Choose a value for n and calculate the UGBW of the auxiliary op-amp (ω_{ua}) required to place the doublet at the location decided in step 2. Obtain the value of current I_1 from the transconductance g_{ma1} which is required to achieve ω_{ua}.
iv. Design a cascode auxiliary op-amp with PFC $C_U = nC_{La}$, having UGBW of ω_{ua} for load capacitance of C_{La} and PM of PM_a. Of course, the dc gain of the op-amp depends on the gain boosting required by the main amplifier.

5 Simulation results

A high-gain moderate-speed low-power fully differential telescopic op-amp is designed in a standard 90 nm CMOS process technology with supply voltage of 1.5 V. The schematic representation of complete op-amp is shown in Fig. 6*a*. On the basis of the above analysis and formulation, the PFC of 100 fF is chosen. Fig. 6*b* shows the magnitude and phase response of the amplifier over the full range of frequencies under consideration with and without PFC across the auxiliary op-amps. Fig. 6*c* shows the same response detailed near the UGBW to understand the deviation of phase and bandwidth in two cases.

The step response of the amplifier is shown in Fig. 7*a* and the simulation results are summarised in Table 2. UGBW and PM of the amplifier increases by 20 MHz and 4°, respectively, when, PFC is connected across the auxiliary op-amps A and B. As a result, ringing in the transient response reduces and 0.01% settling time decreases by 17.5%. For the designed op-amp, the inset shown in Figs. 7*a* and *b* display no significant improvement in the amplifier's time and frequency response when PFC of more than 350 fF is connected across the auxiliary op-amps. The reason behind this is explained in Section 3 where generalised equations and the factor corresponding to the maximum achievable reduction in spacing of the doublet are derived. A 1000 runs Monte Carlo analysis is performed to understand the effect of statistical mismatch on the design. Results of this analysis are shown in Figs. 7*c* and *d*. The standard deviation of 10 MHz and 2.9° in UGBW and PM is within the acceptable range and the design performs satisfactorily under the influence of statistical mismatch.

6 Conclusion

In this paper, a model of the OTA with PFC across the auxiliary op-amp is developed and verified through circuit simulations. The results obtained from circuit simulation and symbolic analysis are in close agreement with each other. It is shown that connecting the PFC across an auxiliary op-amp brings the doublet frequencies closer to each other; however, the effectiveness of the PFC depends on the location of doublet and the targeted application. There is a limitation on improvement in amplifier's behaviour that one can achieve by adding PFC. Employing bigger PFC may not help in terms of design specifications. The design methodology to wisely implement the technique of PFC is presented and a design of high-speed high-gain amplifier is demonstrated. As expected, the results show an improvement in the PM and UGBW of the designed amplifier when PFC is connected across the auxiliary op-amp.

7 Acknowledgments

The authors thank the Department of Electronics and Information Technology (DeitY), Ministry of Electronics and Information Technology (MeitY), New Delhi, Government of India for supporting the work through special man power development – chip to system design (SMDP-C2SD) project. Ashish Joshi would like to extend his gratitude to MeitY for sponsoring this work through Visvesvaraya PhD scheme for Electronics & IT.

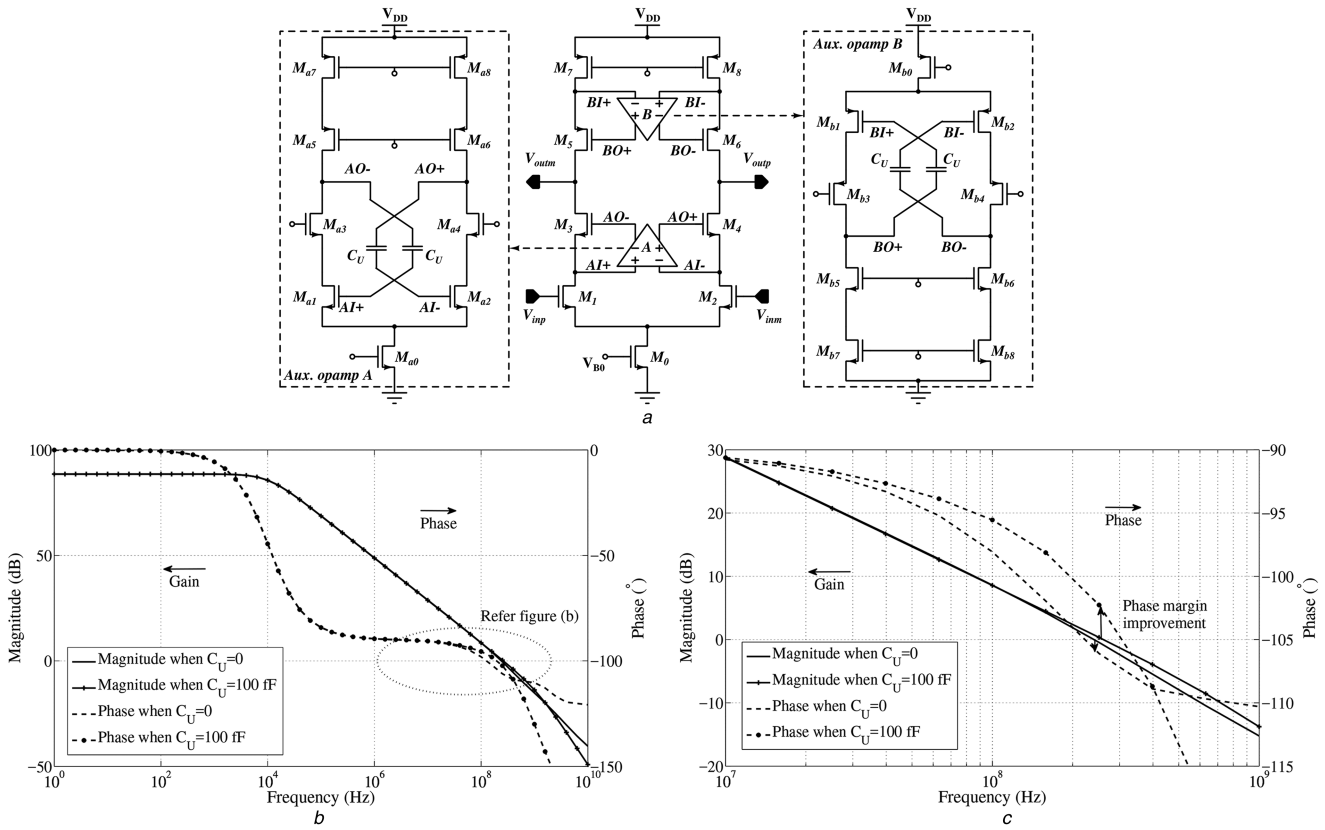

Fig. 6 *Schematic and AC response of the designed amplifier*

(a) Complete schematic representation of the designed gain-boosted amplifier (common mode feedback (CMFB) and bias circuit are not shown here), ***(b)*** Magnitude and phase response of the gain-boosted amplifier with and without PFCs across auxiliary op-amps over full frequency range, ***(c)*** Response zoomed near the UGBW

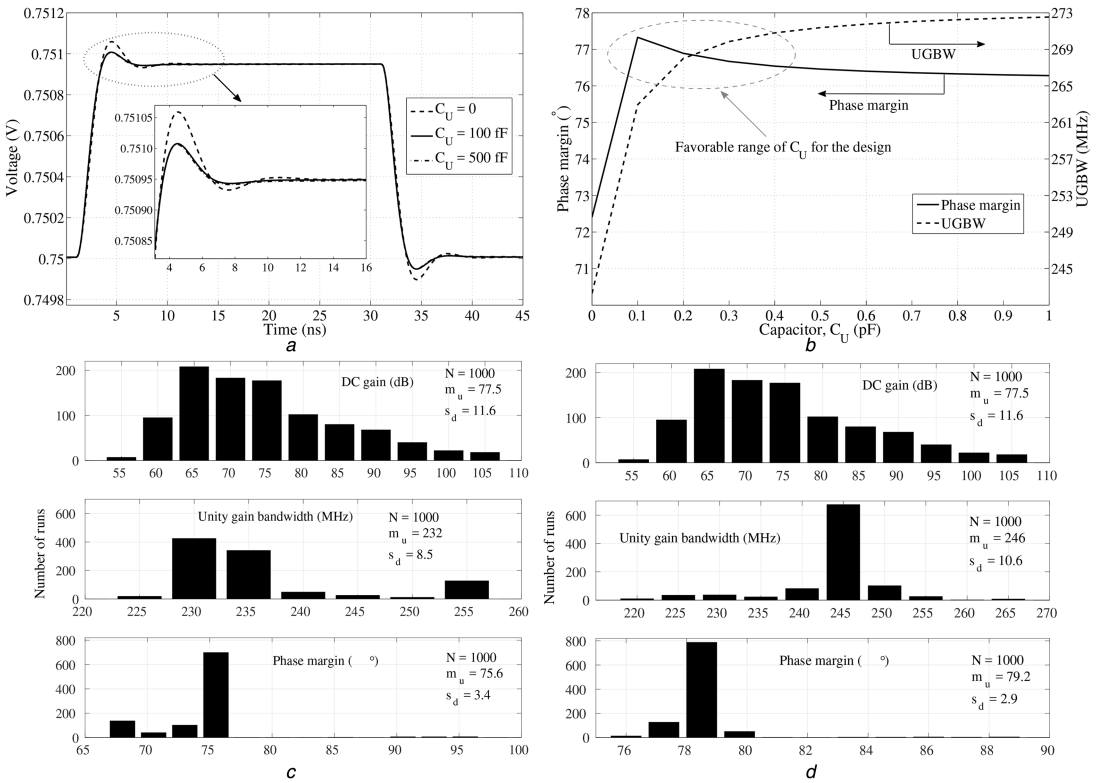

Fig. 7 *Simulation results of the designed amplifier*

(a) Step response of the designed amplifier; settling accuracy of 0.01% is of interest, ***(b)*** PM and UGBW of the designed amplifier for different values of C_U, Monte Carlo analysis when ***(c)*** $C_U = 0$, ***(d)*** $C_U = 100$ fF

Table 2 Summary of the op-amp simulation results

Parameter	Without PFC	With PFC ($C_U = 100\,\text{fF}$)
gain, dB	88	88
UGBW, MHz	242	262
PM, deg	73.41	77.38
0.01% T_{stl}, ns	16	13.2
power, μW	735	735
load capacitance, pF	1	1

8 References

[1] Safi-Harb, M., Roberts, G.W.: 'Low power delta–sigma modulator for ADSL applications in a low-voltage CMOS technology', *IEEE Trans. Circuits Syst. I, Regul. Pap.*, 2005, **52**, (10), pp. 2075–2089

[2] Vecchi, D., Azzolini, C., Boni, A.*, et al.*: '100 MS/s 14 b track-and-hold amplifier in 0.18 μm CMOS'. Proc. of the 31st European Solid-State Circuits Conf. (ESSCIRC), September 2005, pp. 259–262

[3] Devarajan, S., Singer, L., Kelly, D.*, et al.*: 'A 16 b 125 MS/s 385 mW 78.7 dB SNR CMOS pipeline ADC'. IEEE Int. Solid-State Circuits Conf. – Digest of Technical Papers, February 2009, pp. 86–87,87a

[4] Hurrell, C.P., Lyden, C., Laing, D.*, et al.*: 'An 18 b 12.5 MS/s ADC with 93 dB SNR', *IEEE J. Solid-State Circuits*, 2010, **45**, (12), pp. 2647–2654

[5] Gulati, K., Lee, H.-S.: 'A high-swing CMOS telescopic operational amplifier', *IEEE J. Solid-State Circuits*, 1998, **33**, (12), pp. 2010–2019

[6] Kamath, B., Meyer, R., Gray, P.: 'Relationship between frequency response and settling time of operational amplifiers', *IEEE J. Solid-State Circuits*, 1974, **9**, (6), pp. 347–352

[7] Bult, K., Geelen, G.: 'A fast-settling CMOS op-amp for SC circuits with 90 dB DC gain', *IEEE J. Solid-State Circuits*, 1990, **25**, (6), pp. 1379–1384

[8] Das, M., Hellums, J.: 'Improved design criteria of gain-boosted CMOS OTA with high speed optimizations'. IEEE Int. Symp. on Circuits and Systems, Geneva, 2000, vol. **5**, pp. 201–204

[9] Bronskowski, C., Schroeder, D.: 'Systematic design of programmable operational amplifiers with noise-power trade-off', *IET Circuits Devices Syst.*, 2007, **1**, (1), pp. 41–48

[10] Cooley, J.J., Avestruz, A.T., Leeb, S.B.: 'Small-signal analysis of fully-differential closed loop op-amp circuits with arbitrary external impedance elements', *IET Circuits Devices Syst.*, 2011, **5**, (5), pp. 371–383

[11] Flandre, D., Viviani, A., Eggermont, J.-P.*, et al.*: 'Improved synthesis of gain-boosted regulated-cascode CMOS stages using symbolic analysis and *gm*/ID methodology', *IEEE J. Solid-State Circuits*, 1997, **32**, (7), pp. 1006–1012

[12] Aloisi, W., Giustolisi, G., Palumbo, G.: 'Analysis and optimization of gain-boosted telescopic amplifiers'. IEEE Int. Symp. on Circuits and Systems, ISCAS 2002, 2002, vol. **1**, pp. I–321–I–324

[13] Ahmadi, M.: 'A new modeling and optimization of gain-boosted cascode amplifier for high speed and low-voltage applications', *IEEE Trans. Circuits Syst. II, Express Briefs*, 2006, **53**, (3), pp. 169–173

[14] Yang, Y., Binkley, D.M., Li, C.: 'Modeling and optimization of fast-settling time gain boosted cascode CMOS amplifiers'. Proc. of the IEEE SoutheastCon 2010 (South-eastCon), March 2010, pp. 33–36

[15] Nairn, D.: 'Cascode loads and amplifier settling behavior', *IEEE Trans. Circuits Syst. I, Regul. Pap.*, 2012, **59**, (1), pp. 44–51

[16] Singh, P., Debnath, C., Malik, R.*, et al.*: 'Scheme for improving settling behavior of gain boosted fully differential operational amplifier'. US Patent 7,737,780, June 15 2010. Available at http://www.google.co.in/patents/US7737780

[17] Singh, P., Kumar, A., Debnath, C.*, et al.*: '20 mW, 125 Msps, 10 bit pipelined ADC in 65 nm standard digital CMOS process'. IEEE Custom Integrated Circuits Conf., CICC 2007, September 2007, pp. 189–192

[18] Singh, P.N., Kumar, A., Debnath, C.*, et al.*: 'A 1.2 v 11 b 100 Msps 15 mW ADC realized using 2.5 b pipelined stage followed by time interleaved SAR in 65 nm digital CMOS process'. 2008 IEEE Custom Integrated Circuits Conf., September 2008, pp. 305–308

[19] Joshi, A., Yadav, I., Sharma, S.*, et al.*: 'The pole–zero doublet: a cascode operational amplifier with cross coupled capacitor'. 2016 IEEE 59th Int. Midwest Symp. on Circuits and Systems (MWSCAS), Abu Dhabi, United Arab Emirates, 2016, pp. 1–4

[20] '*MATLAB, version 8.6.0 (R2015b)*' (The MathWorks Inc., Natick, Massachusetts, 2015)